Available online at www.sciencedirect.com
ScienceDirect
Tetrahedron: *Asymmetry* 18 (2007) 821–831
Tetrahedron: *Asymmetry*

Preferential crystallization in an unusual case of conglomerate with partial solid solutions

Nicolas Wermester, Eric Aubin, Morgan Pauchet, Servane Coste and Gérard Coquerel*

Laboratoire SMS, UPRES EA 3233, IRCOF, Université de ROUEN, 76821 Mont-Saint-Aignan Cedex, France

Received 11 January 2007; accepted 12 March 2007

Abstract—Ethanolamine mandelate (E.M.) crystallizes as a stable conglomerate and has been found to form partial solid solutions. The crystal structure of the pure enantiomer has been solved from single-crystal X-ray diffraction. In order to determine the extreme compositions of the partial solid solutions in equilibrium (87% ee), the isothermal ternary section in the system [(+)-E.M.–(−)-E.M.–(ethanol–water azeotropic mixture)] was established at 25 °C. Several consecutive preferential crystallization attempts (AS3PC method) were undertaken between $T_B = 41$ °C (starting temperature) and $T_F = 25$ °C (final temperature) on a 2-L scale.

We initially expected to obtain crude crops whose enantiomeric purities would be close to that defined by the isothermal ternary phase diagram (T_F). In fact, the filtered solid phases are of lower enantiomeric excesses: ca. 62% ee. The monitoring of the mother liquor composition over the course of the entrainment shows that the enantiomeric composition of the filtered solid is related to the metastable equilibria involved in the preferential crystallization.

1. Introduction

The pure enantiomers of mandelic acid are of great interest to the chemical industry[1] in general and the pharmaceutical industry in particular. Since the racemic mixture crystallizes as a stable racemate,[2] the optical resolution is usually performed by using the conventional pasteurian method.[3,4] The resolution can also be carried out by means of preferential crystallization (PC) when derivatives such as salts crystallize as conglomerates.[5]

The ethanolamine mandelate salt (E.M., Fig. 1) crystallizes as a stable conglomerate and belongs to the minor fraction of chiral components that also form detectable and stable partial solid solutions.[6] Although previous works[7] have shown that the optical resolution when using the AS3PC process[8] (Auto Seeded Programmed Polythermic Preferential Crystallization) is still applicable, enantiomeric excesses of the crops were lower than anticipated when considering stable equilibria only. As a consequence, the filtered solid could either be a mix of the two stable solid solutions or a single phase in the metastable state. The first case would indicate the nucleation of the opposite solid solution over the course of the entrainment. The latter case can be explained by a traditional approach considering the metastable equilibria.

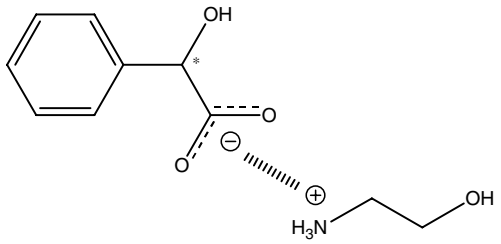

$C_{10}H_{15}NO_4$
M = 213.13 g/mol

Figure 1. Ethanolamine mandelate.

The goal of this study is the characterization of thermodynamic and/or kinetic phenomena that are responsible for such poor purities of the crops.

First, the crystal structure of the pure (*S*)-enantiomer and some molecular modelling considerations are briefly described. Then, the ternary isothermal phase diagram [(+)-E.M.–(−)-E.M.–(ethanol–water azeotropic mixture)] determined at 25 °C is presented. Afterwards, results of several AS3PC attempts performed at a 2-L scale are discussed taking into consideration the metastable equilibria involved in PC.

* Corresponding author. Tel./fax: +33 2 35 52 29 27; e-mail: gerard.coquerel@univ-rouen.fr

0957-4166/$ - see front matter © 2007 Elsevier Ltd. All rights reserved.
doi:10.1016/j.tetasy.2007.03.011

2. Results

2.1. Crystalline structure and molecular modelling

The pure enantiomer of E.M. crystallizes in the widespread $P2_12_12_1$ space group with the following cell parameters at 23 °C: $a = 6.058$ Å; $b = 8.093$ Å; $c = 21.915$ Å. The final cycle of full-matrix least- square refinement on F^2 led to $R_1/wR_2 = 0.030/0.065$ for 1315 unique reflections and 162 parameters. Structure representations are given in Figure 2.

The stability of the crystalline packing is ensured by an extensive network of hydrogen and iono-hydrogen interactions (Fig. 2b and Table 1). The term iono-hydrogen interaction

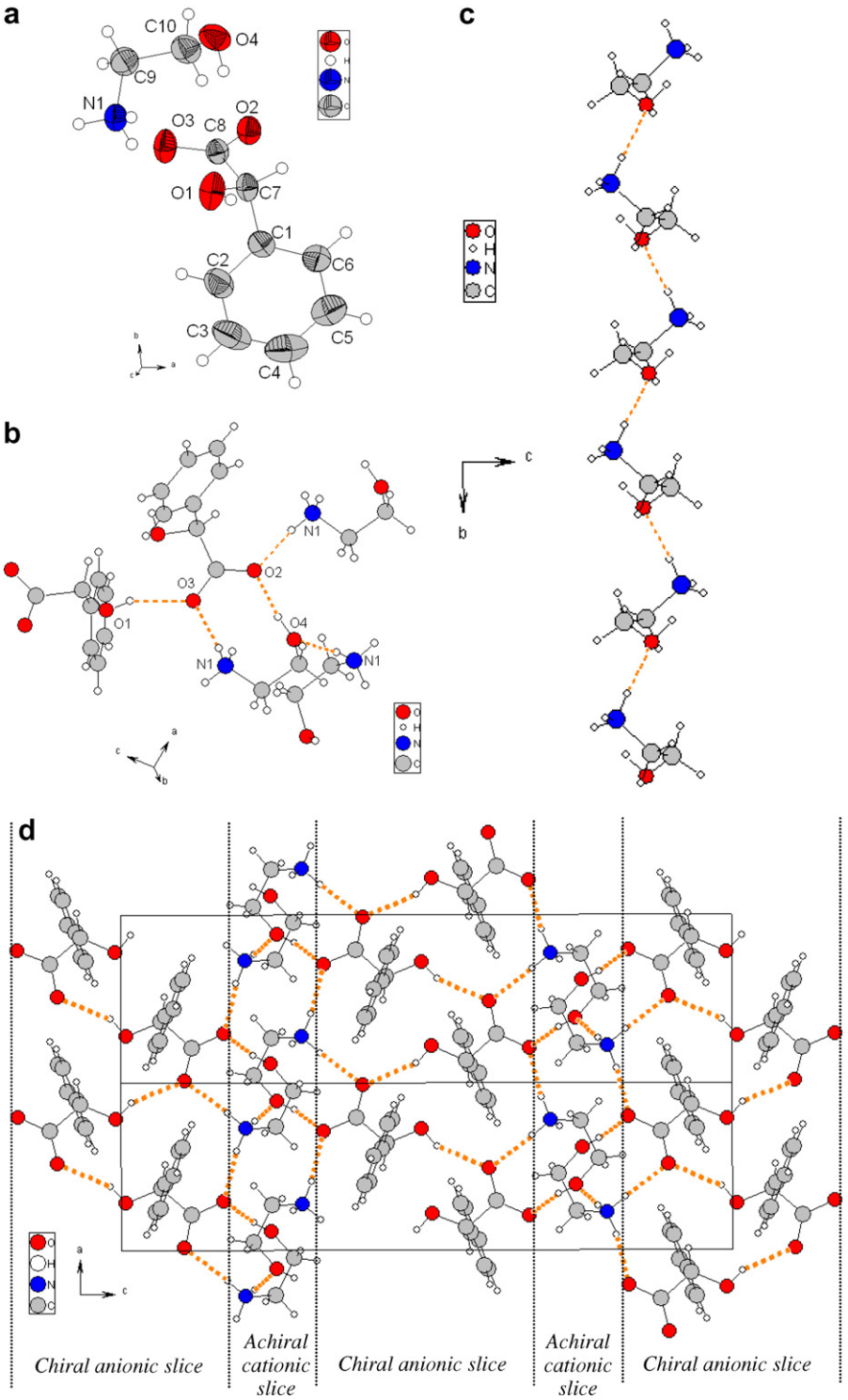

Figure 2. Projections of the crystalline structure of the pure (*S*)-enantiomer of ethanolamine mandelate. (a) ORTEP drawing of the asymmetric unit. (b) Ionic and H-bond network. (c) 1-Dimensional ribbon formed by the ethanolamine molecules along the 2-fold screw axis. (d) Projection of the cell along the *b* axis.

is used to describe a chemical link that exhibits a dual ionic and hydrogen bond character. This is the case for the interaction between O2 and N1 and also between O3 and N1. This phenomenon is related to the mesomeric effect of the carboxylic moiety, confirmed by the quasi equal bond lengths between C8 and the two oxygen atoms: 1.27 Å and 1.24 Å for O2 and O3, respectively. It is worth noting that the ethanolamine molecules are connected by weak hydrogen bonds O4–HN1 and form 1-dimensional ribbons along a 2-fold screw axis (Fig. 2c). These interactions are stabilized by a second hydrogen bond (between the hydroxyl moiety O4H and the oxygen O2 of the mandelic acid) which increases the negative character of the oxygen O4. Besides, the molecules of mandelic acid are connected by the O3–HO1 hydrogen bonds (Fig. 2d), thus forming herring bone like ribbons along $\vec{a}$. The structure can be decomposed into successive slices of chiral anions and achiral cations, parallel to the (0 0 1) plane.

Table 1. Hydrogen and iono-hydrogen bond lengths

Iono-hydrogen bonds	
O2–HN1	1.85 Å
O2–N1	2.73 Å
O3–HN1	1.95 Å
O3–N1	2.80 Å
Hydrogen bonds	
O2–HO4	1.71 Å
O3–HO1	2.07 Å
O4–HN1	1.91 Å

The refinement did not reveal any disorder in this structure.[9] A priori, this packing does not appear to be favourable to the formation of any solid solution, since the stereogenic centre is indirectly connected via strong iono-hydrogen and hydrogen bonds. This rigid and stable packing limits the possibility of molecular disorder, which is usually encountered in solid solutions.

Substantial efforts were made to obtain a suitable single-crystal (size and quality) of a solid solution for X-ray analysis. The presence of the opposite enantiomer seems to induce a significant change in the crystal morphology. It becomes acicular whatever the enantiomeric composition. The thickness of the single-crystals was, however, not sufficient to initiate X-ray measurements.

The crystalline structures of the solid solutions were thus considered by using molecular modelling. Starting from the crystalline structure of the pure enantiomer (Fig. 2), the antipode was generated by inverting the atomic positions of the hydrogen and the hydroxyl moiety (HO1) of the stereogenic centre (C7). This work was carried out on a crystalline packing constituted by nine original cells placed side by side (3 along $\vec{a}$ per 3 along $\vec{b}$). As a first stage, only one enantiomer was substituted in the centre of this packing surrounded by the nonmodified 3-dimensional environment (ee = 94%): by this way, the antipode introduced did not present any periodic interaction with one another. The atomic positions of the inverted atoms (hydrogen and hydroxyl) and lattice energy (molecules were treated as rigid bodies) were successively minimized as described in Section 5. The resulting packing did not show noticeable conformational changes or molecule displacements. The calculated lattice energy is similar to that of the initial packing (pure enantiomer): $\Delta E = +0.3$ kJ/mol, which indicates that, due to the precision of these computations, the stability of such a solid solution cannot be distinguished from that of the pure enantiomer. It is worth noting that the change of the atomic position for the hydroxyl moiety implies the disappearance of the hydrogen bond O3–HO1 (2.07 Å—Table 1) which is replaced by two new others: the first with the hydroxyl moiety of the next mandelic acid molecule along $\vec{a}$ (see Fig. 2d; d(O1–HO1) = 2.14 Å) and the second with a nitrogen atom of an ethanolamine (d(O1–HN1) = 2.18 Å). In the second stage, the same substitution was implemented on half of the mandelic acid ribbon. The resulting ribbon is composed alternatively of (*R*)- and (*S*)-enantiomers, surrounded by their nonmodified 3-dimensional environment (Fig. 2d, 1 modified ribbon over 2 along $\vec{c}$ and 1 over 3 along $\vec{b}$, ee = 84%). The hydrogen bonds are the same as previously described and the lattice energy after minimization is also close to that of the pure enantiomer: $\Delta E = +0.9$ kJ/mol. In the last stage, half of the chiral anionic slices were fully substituted, thus resulting in an alternative stacking of opposite chirality (successive homochiral slices parallel to the (0 0 1) plane, ee = 0%). The lattice energy after minimization is affected by a small decrease: $\Delta E = -3.9$ kJ/mol. From this result, it could be concluded that solid solutions might partially be ordered for compositions close to the racemic mixture (i.e., the existence of racemic clusters composed of successive homochiral slices).[10,11]

Since the variations in lattice energies are small and probably within the range of uncertainty, it can be stated, in a first approximation, that the introduction of the antipode inside the crystalline packing of the pure enantiomer induces only small free enthalpy variations, even for low enantiomeric excesses. Moreover, the Le Bail[12] refinements allowed the estimation of variations of cell parameters between the pure enantiomer and the stable solid solutions (~87% ee). At room temperature, only the crystallographic parameter c seems to present a small but significant decrease for the solid solution (-0.07 Å $\pm$ 0.02 Å). These low variations indicate that there is probably no significant reorganization of the molecules inside the crystalline packing, when one antipode is substituted (this is consistent with the results of the molecular modelling study).

2.2. Thermodynamic characterization of the ethanolamine mandelate system

The binary phase diagram of the enantiomers (Fig. 3b) shows the evolution of the miscibility range at the solid state versus temperature.[7] The maximal composition is ca. 36% ee[†] at 106 °C. The domain width of the solid solutions steeply decreases in a narrow range of temperatures and then remains fairly unchanged on cooling.

Among the usual crystallization solvents, the azeotropic mixture of ethanol (96%) and water (4%, wt %) had been found to be suitable for productive PC. Figure 4 shows

[†] ee stands for enantiomeric excess. ee = $\left|\frac{m_R - m_S}{m_R + m_S}\right|$ with m_R: mass of pure (*R*)-enantiomer in the crude crop and m_S: mass of pure (*S*)-enantiomer in the crude crop.

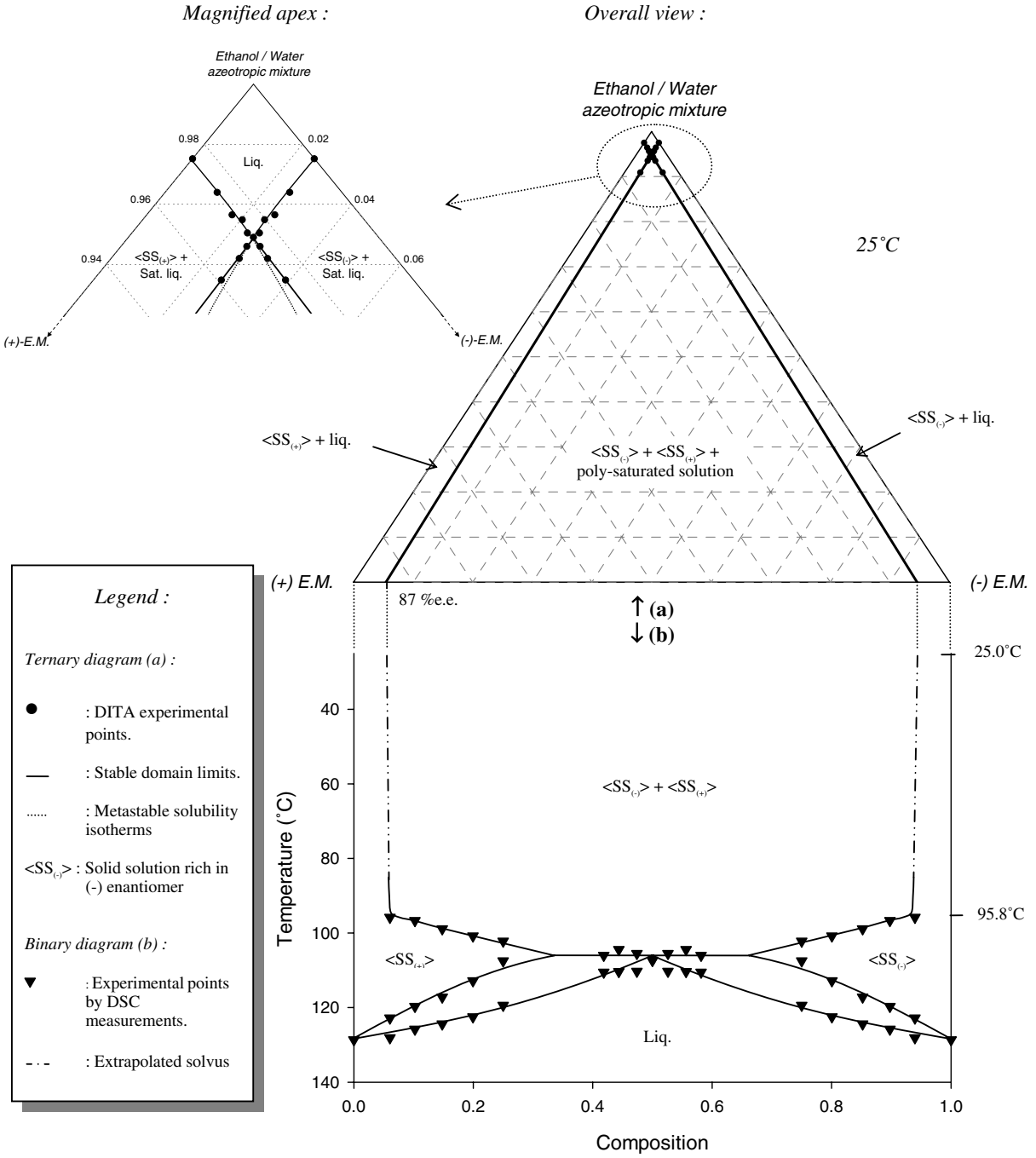

Figure 3. Isothermal section of the ternary phase diagram [(+)-E.M.–(−)-E.M.–(ethanol–water azeotropic mixture)] at 25 °C (a) and binary phase diagram of [(+)-E.M.–(−)-E.M.] (b).

the solubility curve for the racemic mixture as a function of temperature.

An isothermal section ($T = 25$ °C) of the ternary phase diagram [(+)-E.M.–(−)-E.M.–(ethanol–water azeotropic mixture)] is presented in Figure 3. The boundaries of the stable domains were determined by means of DITA measurements (•) (see Section 5). The extrapolation of the two tie-lines down to the bottom axis [(+)-E.M.–(−)-E.M. compositions] allows us to estimate the maximal compositions of the solid solutions at 25 °C: ca. 87% ee. This value is close to that determined by DSC measurements at 95.8 °C: 87.9% ee.

2.3. Auto seeded polythermic programmed preferential crystallization (AS3PC) applied to ethanolamine mandelate

The first AS3PC attempts[7] were performed at a small volume scale (ca. 40 mL) and the entrainment efficiencies were poor ($4.9\% < ee_f$[‡] $< 7.3\%$). The monitoring of mother liquor necessitates several samplings that induce significant and uncontrolled losses of material at this scale.

[‡] ee_f stands for the final enantiomeric excess of the mother liquor at the end of the entrainment.

a

Temperature (°C)	Mass solubility (wt. %)
10.0	2.8
15.0	3.5
20.4	4.2
24.9	5.4
29.7	7.1
34.5	9.3
39.9	12.5
50.3	23.4

b

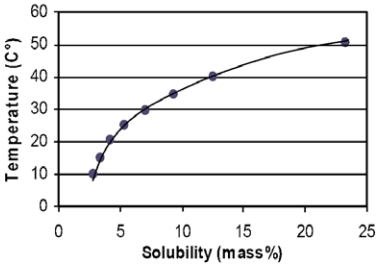

Figure 4. Solubility of (±)-E.M. versus temperature in ethanol (96%, wt %)/water (4%): experimental values (a) and solubility curve (b).[7]

The complementary assays presented here were performed on a larger scale (ca. 2 L), which limited the uncontrolled deviations of the overall composition. Moreover, the volume was also sufficient to implement FBRM® monitoring. It is also worth noting that the stirring was achieved by using a propeller blade (smooth mechanical stirring) avoiding the rubbing effect induced by a magnetic stirring.

Four successive batches were carried out by recycling the mother liquor. The main AS3PC parameters are listed in Table 2. The initial composition of the system for the first run is shown in Table 3.

Table 2. AS3PC parameters

Solvent	Azeotropic mixture ethanol–water (96/4 wt %)
T_B	41 °C
T_F	25 °C
Cooling rate	−0.5 K/min
Solubility $(\pm)_{40\ °C}$	12.5% (wt %)

Table 3. Initial composition of the system

Solvent g/(wt %)	Racemic mixture g/(wt %)	Initial ee g/(ee %)
1 349.4/(87.6)	192.4/(12.4)	8.91/(4.4)[a]

[a] At 41 °C with 4.4% ee, the system in thermodynamic equilibrium is composed of solid solution (ee ⩾ 86%) suspended in the corresponding saturated solution.

Table 4 shows the experimental data for each of the four batches. For batches 3 and 4, the equilibration at $T_B = 41$ °C led to the complete dissolution of the crystals, indicating an increase in solubility. Owing to the hygroscopicity of the system, a low but significant increase in the water/ethanol ratio has been assumed (the solubility of this salt is quite high in water). The starting temperatures T_B were then decreased down to 39.5 °C and 39.0 °C, respectively. These adjustments allowed us to initiate each experiment in accordance with the principles of the auto-seeding procedure (i.e., a partial amount of the enantiomer in excess was already present as a solid crystallized phase at the beginning of the process). For the three first batches, satisfactory final enantiomeric excesses of the mother liquors were obtained ($10.4\% < ee_f < 12.1\%$—Table 4). The best result was obtained for the third run: 53.8 g of crude crop was filtered with an enantiomeric excess of 59.6%. This corresponds to a 32.1 g mass of pure enantiomer. Compared to the previous works, the efficiency of enantiomeric separation has been significantly improved. This observation is due to the change of stirring mode and process scale (the successive samplings did not significantly affect the system).

Figure 5 shows the polarimetric monitoring of the mother liquor for batch 1. From 20 min to 90 min, the inversion of the specific rotation is associated with the entrainment effect. After 90 min, the specific rotation reached a plateau indicating that the slurry had to be swiftly filtered.

Simultaneously, the FBRM® monitoring of the slurry (Fig. 6) clearly shows a two step crystallization process:

- From 20 to 40 min, the number of large particles was slightly increased at the expense of the smaller ones (see Fig. 6, top left part): the supersaturation was low and predominantly crystal growth was occurring.
- After 40 min ($T = T_F = 25$ °C), the FBRM® monitoring shows a sudden surge in the number of fine particles (see Fig. 6, bottom right part): the secondary nucleation rate was high and the viscosity of the slurry was increasing. The concomitant appearance of intermediate sized particles could be associated with aggregation (centre right part) and crystal growth.

Table 4. Experimental conditions and results for the successive AS3PC batches

Batch	Initial ee (%)	T_B (°C)	T_F (°C)	Cooling rate[a] (°C/min)	Time at filtration (min)	Dry crops mass (g)	Crude crops ee (%)	ee_f[b] (%)
1	4.4	41.0	25.0	−0.53	95	45.8	54.9	10.4
2	7.8	41.0	25.0	−0.53	88	41.1	54.4	11.2
3	7.6	39.5	25.0	−0.48	85	53.8	59.6	12.1
4	6.2	39.0	22.0	−0.47	136	83.0	46.3	9.3

[a] The cooling ramp is applied with the indicated rate from T_B to 25 °C. Then, the system is either kept under isothermal conditions (batches 1, 2 and 3) or gradually cooled down to lower temperatures (batch 4—after 115 min).
[b] Calculated for the first batch and measured for the three others.

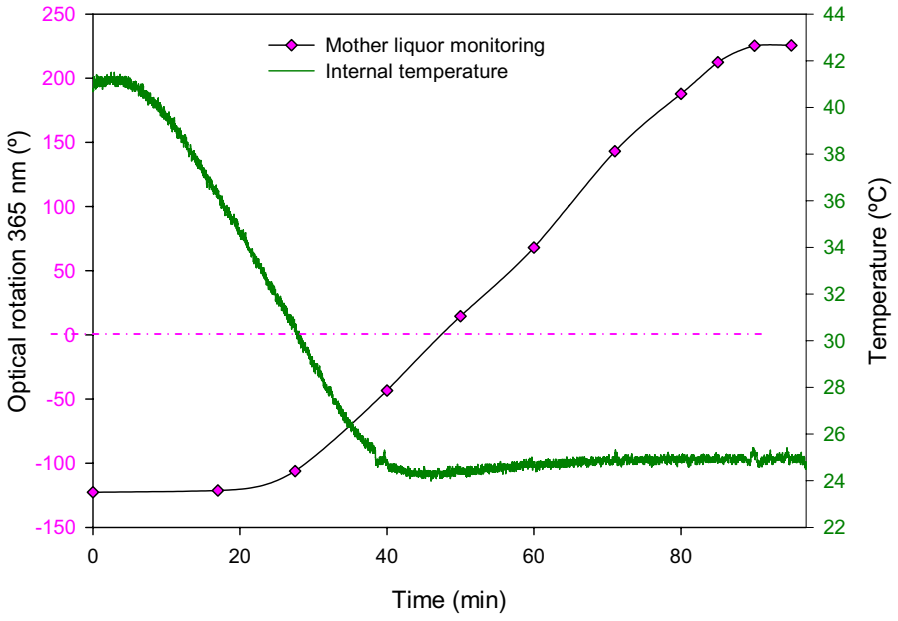

Figure 5. Polarimetric monitoring of the mother liquor during the first AS3PC batch.

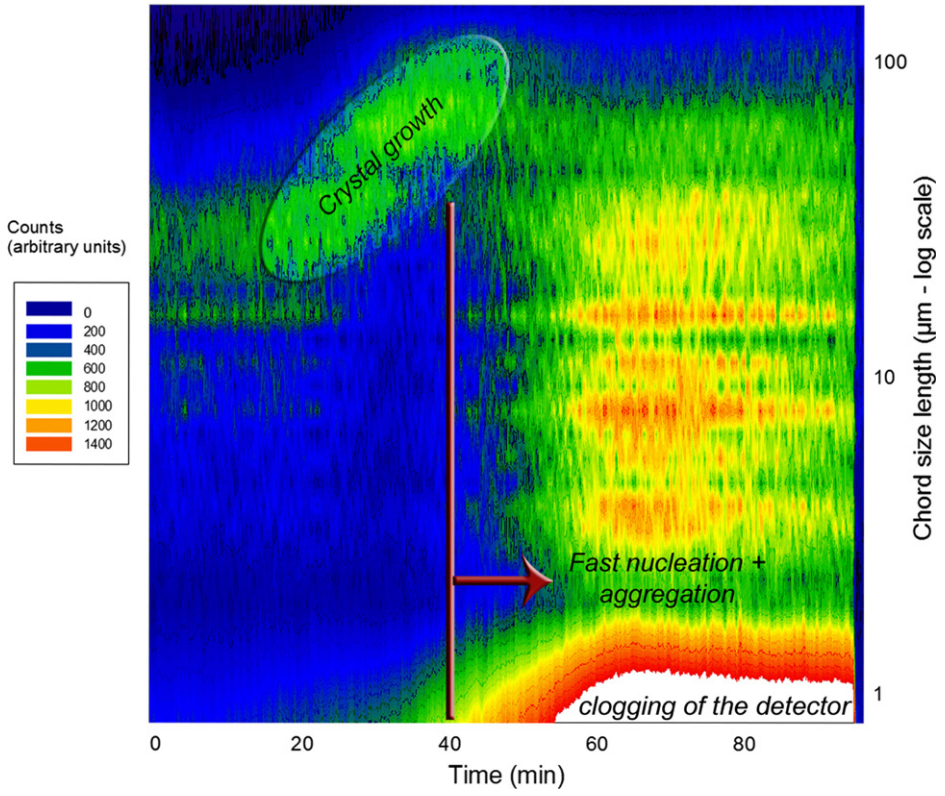

Figure 6. Chord size distribution versus time for the first AS3PC batch.

After 60 min, the FBRM® monitoring was not relevant since an important amount of crystals was stuck on the probe (clogging of the detector). It can be surmised that the number of the smallest particles was continuously increasing. Owing to this poor crystallization kinetics at low supersaturation, the entrainment effect actually started when the cooling ramp was ended. Therefore, AS3PC experiments were performed under quasi-isothermal conditions and thus were not genuine polythermic entrainments. The resulting process is thus similar to the SIPC process,[13]

the only difference being the self-seeding before the application of the cooling ramp.

The enantiomeric excesses of the crops (<60% ee) appeared to be much lower than was anticipated (87% ee at the equilibrium state at 25 °C). This can be rationalized by taking into account the metastable equilibria.

2.4. Metastable equilibria

The ternary phase diagram [(+)-E.M.–(−)-E.M.–(ethanol–water azeotropic mixture)] is of great help in the understanding of the heterogeneous equilibria involved in PC. Over the course of the entrainment, since there is no change in the total composition of the system, the representative point of the overall synthetic mixture (χ point here after—Fig. 7) does not move inside the projection of the phase diagram. Conversely, the boundaries of the crystallization domains move towards the apex of the phase diagram while the temperature is decreased (normal solubilities).

Owing to the 'auto-seeding', at T_B, χ point is located in the stable biphasic domains, that is, $\langle SS_+ \rangle$ plus the saturated solution. The system is in a stable equilibrium.

In order to induce the PC, the temperature is progressively decreased and χ point enters in the stable three-phase domain. Since the mirror image solid solution is not present, the system tends towards a metastable equilibrium involving the domain of crystallization of the initial phase (Fig. 3a).

As previously mentioned, the entrainments were performed under quasi-isothermal conditions. As a consequence, the composition of the crystallizing solid phase is defined by a single metastable tie-line[14] at 25 °C. During the entrainment, the representative point of the liquid phase moves along this tie-line (starting from the vicinity of χ point) and two successive determinations of the mother liquor composition at 25 °C are sufficient to plot it.

In batch 4, mass composition and enantiomeric excess were measured by three substantial samplings as described in Section 5 (Table 5). The resulting points (+) are plotted on the isothermal section of the ternary phase diagram at 25 °C: Figure 8 clearly shows that they are lined up, defining the metastable tie-line of crystallization.

Table 5. Enantiomeric excess and mass composition of the mother liquor samplings at 25 °C during the 4th batch

Sample	Time at sampling (min)	Internal temperature (°C)	E.M. concentration (wt %)	(+)-E.M. enantiomeric excess (ee %)
I	52	25.0	14.41	4.9
II	85	25.0	13.04	−2.1
III	97	25.0	12.43	−5.8

The extrapolation of this tie-line down to the bottom axis (enantiomeric composition) allows the prediction of the enantiomeric excess of the crops at ca. 62% ee (correlation coefficient $R^2 = 0.99997$ in an orthonormal basis). Although this value is close to the enantiomeric purities of the crude crops, they do not perfectly match (Table 4). The experimental purity of the filtration cake results from the significant amounts of mother liquor (of opposite ee) that were trapped inside. Thus, it is normal to obtain crude crops with lower ee than the corresponding ideal enantiomeric excess.

The assessment of the relative mass of solvent trapped (RH hereafter) for each filtration cake allows us to calculate the enantiomeric excess of the solid phase in suspension just before filtration (ee_{JBF}). The general calculation of the

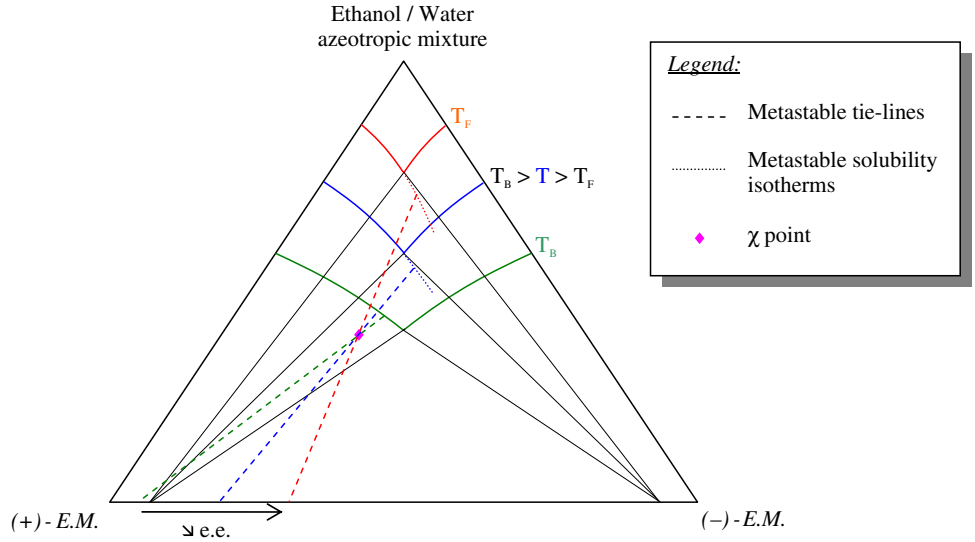

Figure 7. Scheme of the polythermic projection of the ternary phase diagram [(+)-E.M.–(−)-E.M.–(ethanol–water azeotropic mixture)]—from the binary phase diagram (Fig. 3), the maximal composition of the solid solutions at the equilibrium state is supposed to be fairly constant.

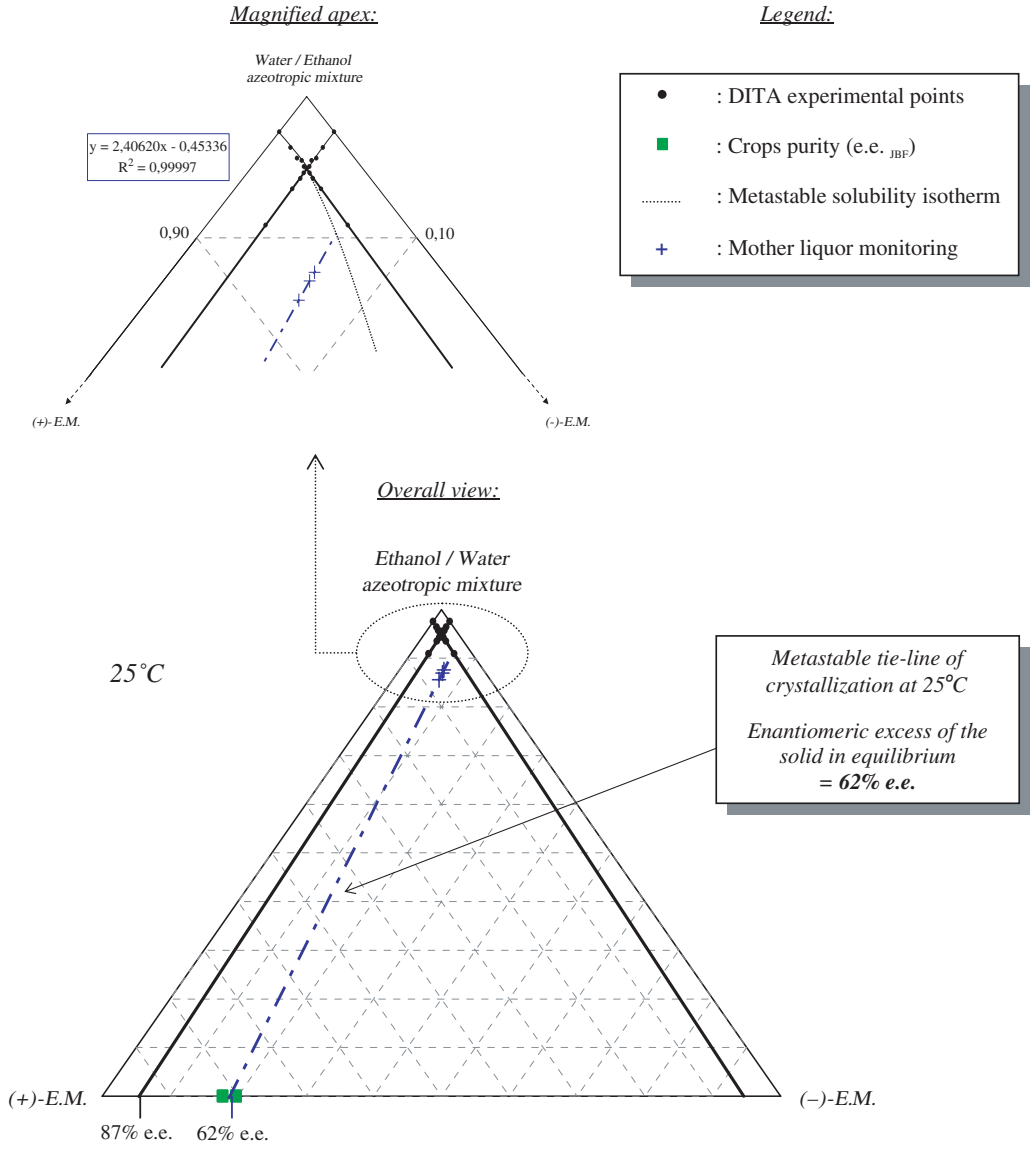

Figure 8. Isothermal section of the ternary phase diagram [(+)-E.M.–(−)-E.M.–(ethanol–water azeotropic mixture)] at 25 °C—determination of the tie-line of crystallization at 25 °C during batch 4.

enantiomeric excess is given by Eq. 1 (where the (*R*)-enantiomer is in excess).

$$\mathrm{ee}_{\mathrm{crop}} = \frac{m_R - m_S}{m_{\mathrm{crop}}} \tag{1}$$

with $\mathrm{ee}_{\mathrm{crop}}$ being the enantiomeric excess of the crude crop, m_R the mass of pure (*R*)-enantiomer in the crude crop, m_S the mass of pure (*S*)-enantiomer in the crude crop and m_{crop} the mass of the crude crop after drying.

In the same way, the $\mathrm{ee}_{\mathrm{JBF}}$ can be calculated by

$$\mathrm{ee}_{\mathrm{JBF}} = \frac{m_{\mathrm{crop}} \times \mathrm{ee}_{\mathrm{crop}} - m_{R\,\mathrm{ad}} + m_{S\,\mathrm{ad}}}{m_{\mathrm{crop}} - (m_{R\,\mathrm{ad}} + m_{S\,\mathrm{ad}})} \tag{2}$$

with $m_{R\,\mathrm{ad}}$ being the mass of pure (*R*)-enantiomer deposited by the mother liquor trapped in the crop and $m_{S\,\mathrm{ad}}$, the mass of pure (*S*)-enantiomer deposited by the mother liquor trapped in the crop.

The analysis of the mother liquor at the end of the run (mass composition and enantiomeric excess) allows us to calculate for each enantiomer the quantity of additional material deposited during drying (Eqs. 3–5)

$$\mathrm{RH} = \frac{m_{\mathrm{wet}} - m_{\mathrm{dry}}}{m_{\mathrm{dry}}} \tag{3}$$

$$m_{R\,\mathrm{ad}} = m_{\mathrm{crop}} \times \frac{\mathrm{RH}}{1-C}\left[C \times \mathrm{ee}_{\mathrm{f}} + \frac{1}{2}(C - C \times \mathrm{ee}_{\mathrm{f}})\right] \tag{4}$$

$$m_{S\,\mathrm{ad}} = m_{\mathrm{crop}} \times \frac{\mathrm{RH}}{1-C}\left[\frac{1}{2}(C - C \times \mathrm{ee}_{\mathrm{f}})\right] \tag{5}$$

with RH being the relative mass of solvent trapped in the crop (expressed as a percentage relative to the dry mass),

Table 6. ee_{JBF} values calculated from Eq. 6 compared with the predicted value

Batch	Dry crops mass (g)	Relative humidity (wt %)	Crude crops ee (%)	Mass concentration[a] of E.M. in the mother liquor (wt %)	ee_{JBF}[b] (%)	Predicted ee (%)
1	45.8	97	54.9	11.1	61.1	62
2	41.1	98	54.4	11.2	60.5	
3	53.8	68	59.6	12.1	64.8	
4	83.0	62	46.3	11.2	55.7	

[a] Calculated for the first batch and measured for the three others.
[b] The parameter C was obtained by calculation for the first batch.

m_{wet}, the mass of the wet cake just after the filtration, m_{dry}, the mass of the dry crop and C, the mass composition of E.M. in the mother liquor.

Finally, the combination of Eqs. 2, 4 and 5 leads to

$$ee_{JBF} = \frac{ee_{crop} - \frac{C}{1-C} \times RH \times ee_f}{(1 - \frac{C}{1-C} \times RH)} \quad (6)$$

The calculated enantiomeric excesses of the solid phases for batches 1–4 are listed in Table 6. The ee_{JBF} of the crops for batches 1–3 are consistent with the predicted value. This indicates that there was probably no important nucleation of the opposite solid solution over the course of these three entrainments. For batch 4, it is worth noting that the final temperature needed to be decreased ($T_F = 22$ °C) inducing a significant drop of the enantiomeric excess. This could be related to at least three nonexclusive reasons: (i) the metastable tie-line at 22 °C is different from that at 25 °C; (ii) the uptake of water might also have an impact in the stereoselectivity of the crystallization; (iii) the possible nucleation of the antipode.

3. Discussion

The final enantiomeric excesses of the mother liquors ($ee_f > 10\%$) showed that AS3PC works well for this system. Despite the high supersaturations necessary for any substantial crystal growth, the three first entrainments were not interrupted by the nucleation of the antipode. This is consistent with the absence of metastable racemic compound of close stability or epitaxy phenomenon between crystals of the two enantiomers. The efficiency of the enantiomeric separation is rather limited by the solid solutions. The enantiomeric purity of the crops could be improved by adjusting T_B close to T_L: it is expected that at least 40% of the crops could be crystallized in the stable two-phase domain with an enantiomeric excess superior to 87%. Nevertheless, the complete optical resolution would necessitate additional processing steps (salting out, recrystallization(s) and preparation of other derivatives…) in order to access to high ee with a substantial yield.

This study has demonstrated that the metastable equilibria involved in PC are responsible for the low enantiomeric purities of the crops when solid solutions exist. Otherwise, molecular modelling has shown that the lattice energy variation as a function of the enantiomeric purity does not seem to be steep. This is consistent with both: the existence of the symmetrical stable solid solutions and the orientation of the metastable tie-lines (at low supersaturations, the enantiomeric excess of the solid in metastable equilibrium with its mother liquor decreases significantly, see Fig. 8).

As shown in Figure 7, the enantiomeric excess of the solid phase in metastable equilibrium decreases with the temperature. Since the diffusion kinetics at the solid state is very low and not significant for the time scales of our experiments,[15] it can be postulated that along the PC process, slight changes only occur in the composition of the solid solutions. This could induce the formation of enantiomeric gradients inside the crystalline particles. The thermodynamic approach using phase diagrams does not take into consideration these kinetic effects (the solid phase composition is considered to be homogeneous and in equilibrium for each temperature).

Although the PC attempts were performed under quasi-isothermal conditions, a complementary experiment was carried out to determine if the composition of the solid particles was really homogeneous: a part of the third batch crop has been progressively dissolved by successively passing through the solid phase 15 mL of ethanol–water azeotropic mixture. Then, the quantities of dissolved masses and their enantiomeric excesses were determined by means of gravimetric methods and polarimetric measurements. It should be noted that the crop was smoothly sieved beforehand in an attempt to eliminate the smallest particles (<200 μm). Figure 9 shows the ee as a function of the cumulated dissolved mass. This experiment was repeated twice, leading to similar results.

Despite preliminary sieving, the first dissolved material is affected by a low enantiomeric excess ($53\% < ee_{JBF}$), which is likely to indicate the residual presence of crystals deposited during the drying of the crop ($ee = ee_f = -12.1\%$): this could be related to the formation of aggregates that might trap a significant amount of fines. Although the enantiomeric excess of the major part of the crystalline mass is close to that predicted, this representation clearly demonstrates that an enantiomeric gradient exists inside the largest crystalline particles. While dissolving, the composition of the crystals gets closer to the enantiomeric composition at T_B. However, the purity of the last fraction does not reach the enantiomeric purity defined at T_B (>87% ee). This could indicate the beginning of the diffusion at the solid state during the 90 min of the PC or an insufficient equilibration time at T_B (since a quench was beforehand applied—see Section 5).

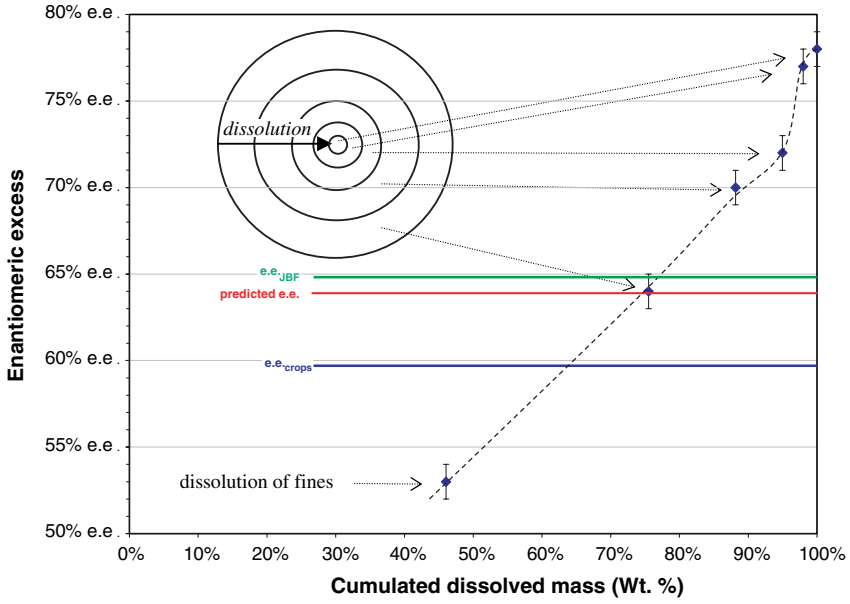

Figure 9. Evolution of the ee of the dissolved solid as a function of the cumulated dissolved mass (batch 3)—the calculated barycentre of the values (ee, dissolved mass) corresponds to the ee_{crops} (60%).

4. Conclusion

In the context of the optical resolution, the existence of solid solutions between enantiomers is an additional factor limiting the interest of preferential crystallization methods. However in this particular case, the entrainment efficiency is satisfactory. Thus, it has to be dissociated from other systems involving a metastable racemic compound[16] or epitaxy phenomena[17] for which the PC is hardly applicable. Obviously, the efficiency of entrainments has to be evaluated by assessing the ee_f parameter (i.e., the enantiomeric excess which is attainable at the end of the process) and not from the enantiomeric purities of the crops.

This study demonstrated that the knowledge of the stable equilibria is not sufficient enough to determine the purity of the crops that depends on the orientation of the metastable tie-lines. One can imagine a case where the stable equilibrium indicates a maximum composition near 100% ee, whereas the metastable equilibria involve solid phases of much lower purities. In all cases, the adjustment of T_B close to T_L should improve the average enantiomeric purity of the crops when using the AS3PC variant of the preferential crystallization.

Crystallographic data have been deposited at the Cambridge Crystallographic Data Center (CSD) and registered under the deposition number 613397.

5. Experimental

Ethanolamine mandelate salts were formed using mandelic acid (99% ee and racemic mixture) and ethanolamine (99% purity) purchased from Acros Organics®. All batches of salts were prepared following the same procedure: A clear solution of mandelic acid was first prepared in acetone (p.a.). Then, a stoichiometric mass of pure ethanolamine (liquid state at ambient temperature) was slowly added (while stirring) leading to the spontaneous crystallization of the salt after few minutes. Finally, the filtration of the slurry was carried out on a glass filter number 4.

The crystal structure of the pure enantiomer was determined from single-crystal X-ray diffraction on a Bruker® SMART APEX diffractometer (with $Mo_{K\alpha 1}$ radiation: 0.71073 Å). E.M. structure was solved by means of the direct methods and refined with the SHELXTL® package.[§] Single-crystals were obtained by a slow evaporation of a saturated solution (water–ethanol azeotropic mixture).

Molecular modelling was used to study the enantiomeric substitution on a molecular scale. The lattice energies were minimized by using the 'smart minimizer' module of Cerius^2 software[¶] with a standard convergence (maximum of 500 iterations, never reached, stop at $\frac{\Delta E}{E} = 10^{-3}$ kJ/mol). Dreiding[18] force field 2.21 was used and MOPAC charges[19] using the AM1 method were assigned to the atoms. Ewald summations were carried out on both Coulombic and van der Waals interactions. As a first step, energy minimization was carried out on the structure of the pure enantiomer (molecules were treated as rigid bodies), which induced a decrease in the density due to significant changes of the cell parameters: $\Delta a = 0.43$ Å; $\Delta b = 0.51$ Å; $\Delta c = -1.76$ Å. These variations are related to the nature of the modelling parameters (principally force field and charges calculation) that were obviously not optimized for this specific case. Nevertheless, the resulting lattice energy was chosen as the reference for the comparison of stabilities.

[§] SHELXTL V6.10 (2000), Xshell user's manual, Bruker Advanced X Ray Solutions, Inc., Madison, Wisconsin, USA.

[¶] Cerius^2, Accelrys Inc., version 4.6, Cambridge, UK, website: www.accelrys.com.

Le Bail[12] refinements were realized by using WinPLOTR software[20] (Thomson-Cox-Hastings profile function).[21]

X-ray powder diffraction measurements were carried out by using a SIEMENS D5000 Matic diffractometer (Bruker analytical X-ray Systems, D-76187 Karlsruhe, Germany) with a Bragg Brentano geometry, in theta–theta reflection mode. The instrument is equipped with an X-ray tube (copper anticathode, 40 kV, 40 mA, $K_{\alpha 1}$ radiation: 1.540598 Å, $K_{\alpha 2}$ radiation: 1.544426 Å), a nickel filter and a scintillation detector. The diffraction patterns were collected by steps of 0.04° (2-theta) over the angular range 3–30°, with a counting time of 4 s per step. No internal standard was used but a sample of quartz was analyzed as an external standard. The analyses were carried out at room temperature. DIFFRAC PLUS Edit Job software[‖] was used as control software and data processing was performed by using the Eva software.[††]

The isothermal ternary phase diagram [(+)-E.M.–(−)-E.M.–(ethanol–water azeotropic mixture)] at 25 °C was established by means of DITA (Discontinuous Isoperibolic Thermal Analysis)[22–24] measurements.

Polarimetric measurements were performed with a Perkin–Elmer® No. 341 ($\lambda = 365$ nm, $T = 25$ °C, $l = 10$ cm).

FBRM® measurements (Focussed Beam Reflectance Measurements technique – chord length from 0.8 to 1000 μm—Metler Toledo®) were used to determine the chord size distribution of the solid particles during the course of the entrainments.

Thermal analyses were carried out by using a Setaram® 141 Differential Scanning Calorimeter. No purge gas was used. The reference material was an empty aluminium pan without a cap. The samples were weighed in open aluminum pans and then placed in the analyzer. The analyses were performed within various temperature ranges using a 1 K min^{-1} heating rate.

Preferential crystallizations using the Auto-Seeded variant (AS3PC[25]) were performed in a 2-L double-wall reactor. Temperature was accurately controlled by a cryo/thermostat (Huber® polystat CC3) and the internal temperature versus time was recorded. The mixture was stirred with a marine propeller (200–300 rpm—diameter 8 cm—stainless steel). Starting with a homogeneous solution ($T \gg T_B$), a quench was first applied to obtain fine particles. Then, the system was kept at T_B for at least one hour to ensure that the suspension contained only particles of one solid solution. The auto-seeded PC was then ready to be started. The course of the entrainment was monitored by off-line polarimetric measurements of the mother liquor: the presence of very small particles required a filtration prior measurement with disposable Gelman® Acrodiscs media (0.45 μm). At the same time, the clear mother liquor was sampled to determine its global composition (mass concentration) by the mean of the usual gravimetric method. The crystallization kinetics was monitored by continuous in-line chord size distribution measurements (FBRM®).

At the end of the entrainment, the slurry was filtered by depression at room temperature (glass filter number 4—diameter 19 cm). The filtration cake was neither washed nor re-crystallized. The enantiomeric purities of the crops were determined by polarimetry. For each batch, the final composition of the mother liquor was measured (mass concentration and ee_f = enantiomeric excess of the mother liquor at the end of the run). In order to start a new run, the lost material was replaced by adding the racemic mixture and solvent.

[‖] DIFFRAC PLUS version 2.0, copyright®.

[††] EVA version 9.0.0.02, copyright® SOCABIM, 1996–2003.

References

1. Mill, J.; Schmiegel, K. K.; Shaw, W. N.; U.S. Patent, 4391826, 1983.
2. Lorenz, H.; Seidel-Morgenstern, A. *Technica Acta* **2004**, *415*, 55–61.
3. Pasteur, L. *C.R. Acad. Sci.* **1853**, *37*, 162.
4. Pasteur, L. *Ann. Chim. (Paris)* **1853**, *3*, 457.
5. Jacques, J.; Collet, A.; Wilen, S. H. *Enantiomers, Racemates and Resolutions*; Kriger: Malabar Florida, USA, 1994.
6. Coquerel, G. *Enantiomer* **2000**, *5*, 481–498.
7. Aubin, E.; Petit, M.-N.; Coquerel, G. *J. Phys. IV France* **2004**, *122*, 157–162.
8. Coquerel, G.; Petit, M.-N.; Bouaziz, R.; PCT Patent, WO 95/08522; see also Coquerel, G. Novel Optical Resolution Technologies. In *Topics in Current Chemistry*; Sakai, K., Hirayama, N., Tamura, R., Eds.; Springer: Berlin/Heidelberg, 2006; Vol. 269.
9. Banerjee, R.; Bhatt, P. M.; Krichner, M. T.; Desiraju, G. R. *Angew. Chem., Int.* **2005**, *44*, 2515–2520.
10. Lajzerowicz, Ja.; Chion, B.; Lajzerowicz, Jo. *J. Chem. Phys.* **1981**, *74*, 3500–3509.
11. Lajzerowicz, Ja.; Lajzerowicz, Jo.; Bordeaux, D. *Phys. Rev. B* **1986**, *34*, 6453–6463.
12. Le Bail, A.; Duroy, H.; Fourquet, J. L. *Mater. Res. Bull.* **1988**, *23*, 447–452.
13. Collet, A.; Brienne, M.-J.; Jacques, J. *Chem. Rev.* **1980**, *80*, 215.
14. Ricci, J. E. *The Phase Rule and Heterogeneous Equilibrium*; Dover, 1966; pp 21–24.
15. Matovic, M.; Van Miltenburg, J.-C.; Los, J. *J. Cryst. Growth* **2005**, *275*, 211–217.
16. Dufour, F.; Perez, G.; Coquerel, G. *Bull. Chem. Soc. Jpn.* **2004**, *77*, 79–86.
17. Gervais, C.; Beilles, S.; Cardianel, P.; Petit, S.; Coquerel, G. *J. Phys. Chem.* **2002**, *106*, 646–652.
18. Mayo, S. L.; Olafson, B. D.; Goddard, W. A. *J. Phys. Chem.* **1990**, *94*, 8897–8909.
19. Stewart, J. J. P. *Comput. Aided J. Mol. Des.* **1990**, *4*, 1–105.
20. Roisnel, T.; Rodriguez-Carvajal, J. *Mater. Sci. Forum* **2001**, *118*, 378–381.
21. Thomson, P.; Cox, D. E.; Hastings, J. B. *J. Appl. Cryst.* **1987**, *20*, 79–83.
22. Marchand, P.; Lefèbvre, L.; Courvoisier, L.; Counioux, J.-J.; Coquerel, G. *J. Phys. IV France* **2001**, *11*, 115–122.
23. Marchand, P.; Lefèbvre, L.; Perez, G.; Counioux, J.-J.; Coquerel, G. *JTAC* **2002**, *68*, 37–47.
24. Marchand, P.; Lefèbvre, L.; Querniard, F.; Cardinael, P.; Perez, G.; Counioux, J.-J.; Coquerel, G. *Tetrahedron: Asymmetry* **2005**, *15*, 2455–2465.
25. Ndzié, E.; Cardinael, P.; Schoofs, A.-R.; Coquerel, G. *Tetrahedron: Asymmetry* **1997**, *8*, 2913–2920.